Determination of Critical Indices by "Slow" Spectroscopy: NMR Shifts by Statistical Thermodynamics and Density Functional Theory Calculations

Vytautas Balevicius,*,† Vytautas Juozapas Balevicius,† Kestutis Aidas,† and Hartmut Fuess‡

Faculty of Physics, Vilnius University, LT-10222 Vilnius, Lithuania, and Institute of Materials Science, University of Technology Darmstadt, D-64287 Darmstadt, Germany

Received: August 24, 2006; In Final Form: November 27, 2006

The temperature dependencies of NMR shifts in the critical region of two coexisting phases have been simulated using statistical thermodynamics and graph-theory consideration of equilibrium processes of molecular association. *Micro*parameters of magnetic screening of various water and water/pyridine structures used in the statistical averaging have been evaluated by density functional theory calculations (PBE1PBE and B3PW91 functionals in the 6-311++G** basis set). The gauge-including atomic orbital (GIAO) approach has been applied to ensure gauge invariance of the results. Solvent effects were taken into account by a polarized continuum model (PCM). NMR shifts "order parameters" ($\Delta\delta = |\delta^+ - \delta^-|$) and "diameters" ($\phi\delta = |(\delta^+ + \delta^-)/2 - \delta_C|$, where δ^+, δ^-, and δ_C are the chemical shifts of coexisting phases and at the critical point respectively) have been calculated in each case close to the lower critical solution point (T_L) and processed using linear regression analysis of $\Delta\delta \sim |T - T_L|$ and $\phi\delta \sim |T - T_L|$ in the log–log plot. It has been shown that the critical index β can be evaluated with high precision from the slope of $\Delta\delta = f(T - T_L)$ at any realistic set of model input parameters. The slope of diameter has been found to depend on both input β and α values. The obtained $\phi\delta$ slopes (0.58–0.63) are very close to 2β values. The results are discussed within the concept of complete scaling. Results of simulation are compared and supported by experimental NMR data for water/2,6-lutidine, acetic anhydride/*n*-heptane, and acetic anhydride/cyclohexane systems.

I. Introduction

Critical indices and critical amplitudes are those crucial and universal parameters that reflect most peculiarities of physical systems close to their phase transition point.[1,2] Among the most intriguing findings in this field in recent years were the discovery of crossover between the solvophobic and ionic critical regimes,[2,3] multiple critical points,[4,5] and nonequilibrium restructuring phenomena.[6,7] Despite very precise and exhaustive studies, several open questions persist, and some conclusions are even controversial.

Hence, new convenient experimental ways to determine various critical parameters based on "easily measurable" quantities are of high scientific and practical value. A concept to establish a relationship "critical parameter" ↔ "easily measurable quantity" requests a theoretical background. Such a concept would, first of all, support the existence of correlations of this kind, and furthermore, it should determine physical margins of their validity.

Most spectral parameters (vibrational frequencies, band intensities, NMR chemical shifts, etc.) can be considered as those easily measurable quantities. Exceptional cases may exist, e.g., analysis of complicated vibrational band shapes in systems with very strong H-bonds,[8] or NMR spectra of nuclei of low natural abundance, when a huge amount of data has to be sampled and processed.[9]

Nevertheless NMR chemical shifts are indeed parameters that can be measured with very high accuracy, even in the region of critical fluctuations.[10–14] NMR shifts of nuclei directly involved in the most important interactions, e.g., hydrogen bonding, dipole–dipole aggregation, clustering, etc. that fate the major structural features of the system, are extremely sensitive to temperature and composition changes. Thus they can be considered as the main source of information studying critical phenomena. NMR is, however, in a dynamical sense a "slow" spectroscopy. This means that measured NMR shifts are averaged over numerous spatial manifolds in the system (various associates, clusters, conformations, etc.), and hence, some features and parameters of critical behavior are "hidden" in this averaging procedure. The main challenge could be formulated as "what are the chances to extract certain information on critical parameters applying physical techniques, that on the one hand are slow in time scale of molecular processes, but on the other hand, provide a huge and precise set of necessary data to be collected in short time experiments?" A suitable way to determine critical indices based on the temperature-dependence of NMR chemical shift is proposed in the present work. Statistical thermodynamics and graph theory considerations were applied to describe processes of chemical equilibrium of association of molecules, and the quantum chemical density functional theory was used to evaluate individual properties (magnetic screenings) of various molecular structures.

II. Graph Theory and Thermodynamics of Molecular Association

The mathematical methods of topology and graph theory are widely used solving very sophisticated cases of molecular structure features, kinetics of chemical reactions, chemical equilibrium, etc.[15,16] Complicated molecular processes, chemical

* Corresponding author phone: 370 5 2366 040; fax: 370 5 2366 003; e-mail: vytautas.balevicius@ff.vu.lt.
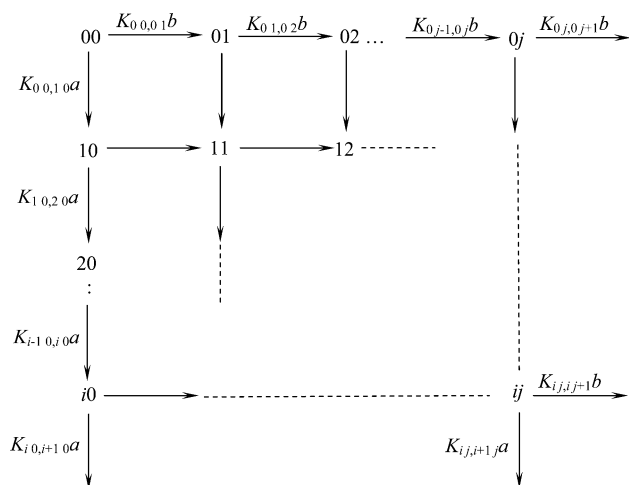† Vilnius University.
‡ University of Technology Darmstadt.

Figure 1. Directed graph of chemical equilibria (1). $K_{ij,kl}$ are the equilibrium constants of elementary (one-edge) reactions, a and b are the mole fractions of nonbonded molecules A and B respectively. More comments in text.

equilibria among them, take place in many critical systems, and as a rule, one of the components involved is water.[1-7] Indeed, molecular association processes should be treated in these cases using the most general scheme, including a set of chemical equilibrium reactions of components A and B:

$$i\text{A} + j\text{B} \leftrightarrow \text{A}_i\text{B}_j, \ (i,j = 0, \dots, \infty) \tag{1}$$
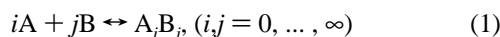
and a set of corresponding equilibrium constants. Note that this scheme has been successfully applied studying stacking interactions and association of molecules in some biologically active systems by NMR spectroscopy.[17-19]

Some useful tools to consider chemical equilibrium processes, developed in graph theory,[16,17] will be applied for a general case of eq 1. For this purpose, a set of reactions (1) is symbolically represented by a directed graph (Figure 1).

Vertices of the graph correspond to molecular associates A_iB_j, i.e., their stoichiometrie determined by indices of vertices ij. Each directed edge represents, in this case, an elementary stage of the attachment either of A (vertical edges) or B (horizontal edges) molecules with corresponding equilibrium constants.

The basic statement for NMR data analysis is that the reaction of magnetic moments of nuclei upon molecular motion can be neglected. In other words, the spin states are transported between spatial states with spin-independent rates. The average values of parameters of a spin-Hamiltonian (magnetic screenings, spin couplings constants) due to the fast chemical exchange is therefore given by

$$\langle \delta \rangle = \sum_i p_i \delta_i \tag{2}$$

where δ_i is the value of the corresponding spin-parameter in the ith spatial manifold, and p_i is the probability of the system in that manifold. Note that such a relationship between *macro-* and *micro-*features of the system is valid also for many properties measured in other physical experiments (e.g., extinction coefficients, reaction cross-sections, etc.).

The relation (eq 2) in the directed graph treatment can be rewritten using Mason's rule[17] as follows:

$$\langle \delta \rangle = \sum_{i,j} D_{ij}\delta_{ij} / \sum_{i,j} D_{ij} \tag{3}$$

where D_{ij} is the determinant of ij-vertex, and δ_{ij} is a *micro-*parameter of the aggregate A_iB_j (e.g., its NMR signal shift).

The D_{ij} are defined as the sum of possible routes from the 00-vertex (a standard state) to the ij-vertex. The consecutive edges in each path are linked multiplying their lengths, and the parallel paths are added. Let us demonstrate this routine starting from the vertices of lowest order:

$$D_{00} = 1 \ (\text{arbitrary});$$
$$D_{01} = D_{00}K_{00,01}b = K_{00,01}b; \ D_{10} = K_{00,10}a;$$
$$D_{11} = K_{00,01}bK_{01,11}a + K_{00,10}aK_{10,11}b; \ D_{12} = D_{11}K_{11,12}b + $$
$$D_{01}K_{01,02}bK_{02,12}a; \ \dots$$

Taking into account the thermodynamic relation between equilibrium constant (K) and the change of Gibbs free energy (G) as $K = \exp\{-[G(\text{final state}) - G(\text{initial state})]/RT\}$ the above expressions can be simplified as follows:

$$D_{11} = \{K_{00,01}K_{00,11} + K_{00,10}K_{10,11}\}ab = $$
$$\{\exp[-(G_{01} - G_{00})/RT] \exp[-(G_{11} - G_{01})/RT] + $$
$$\exp[-(G_{10} - G_{00})/RT] \exp[-(G_{11} - G_{10})/RT]\}ab = $$
$$2 \exp[-(G_{11} - G_{00})/RT]ab$$

and in the same way

$$D_{12} = 3 \exp[-(G_{12} - G_{00})/RT]ab^2$$

Generalizing these rules leads to

$$D_{ij} = \binom{i+j}{i} K_{ij}a^i b^j \tag{4}$$

where $\binom{i+j}{i}$ are binomial coefficients, K_{ij} is the total equilibrium constant, step by step composed of equilibrium constants of elementary reactions $K_{ij,kl}$. The total equilibrium constants K_{ij} are related to corresponding changes of thermodynamic parameters related to the formation of A_iB_j with respect to a standard state $\Delta G_{ij} = G_{ij} - G_{00}$ (Gibbs free energy), ΔH_{ij} (enthalpy) and ΔS_{ij} (entropy):

$$K_{ij} = \exp(-\Delta G_{ij}/RT) = \exp(-\Delta H_{ij}/RT + \Delta S_{ij}/R) \tag{5}$$

The quantities a and b are the mole fractions of nonbonded molecules A and B (monomers) respectively, and they are found by solving the balance equations for both components:

$$\sum_{i,j=1}^{\infty} iD_{ij} = x_\text{A}$$

$$\sum_{i,j=1}^{\infty} jD_{ij} = x_\text{B} \tag{6}$$

where x_A and x_B are the total mole fractions of A and B molecules in solution. Hence, in the case of a two-component system, $x_\text{A} + x_\text{B} = 1$.

These quite general relations (3-6) can be adapted for modeling the critical behavior of NMR shifts (3) by inserting

into (6) a proper asymptotic expansion of concentration along the phase coexistence boundary, like

$$x = x_c \pm B_0|t|^\beta + B_a|t|^{1-\alpha} + ... \qquad (7)$$

where $t = (T - T_c)/T_c$ is the reduced temperature, T_c, x_c, B_0, B_a, α, β are the critical parameters: temperature, concentration, amplitudes, and indices, respectively. Exact formulas and values of critical indices and critical amplitudes for many interesting systems obtained from light scattering, refractive indices, density, and viscosity measurements are presented in refs 1, 20−22.

To simplify the modeling any restraints on model input parameters are desirable. One of these might be an entropy term in eq 5, which has to be treated in more detail. First of all, the binomial coefficient factor in eq 4 determines a permutational contribution to the total entropy change:

$$\Delta S_{\text{permut}} = R \log\binom{i+j}{i} = R \log \frac{(i+j)!}{i!j!} \qquad (8)$$

During the growth of a stack A_iB_j successive additions of next molecules should be increasingly less probable and hence less favored entropically. This contribution (a stacking contribution) can be scaled as

$$\Delta S_{\text{stack}} = R \log \frac{1}{(i+j)!} \qquad (9)$$

and, applied together with ΔS_{permut}, it leads to an extension of the so-called *attenuated constants model*, analyzed in ref 17. The main idea of this model in terms of graph treatment is that an elementary step equilibrium constant $K_{i-1,i}$ (constant of *homo*-association) varies along $10 \rightarrow 20, \rightarrow ... \rightarrow i0 ...$ (i.e., $j = 0$) edges as $\sim 1/i$. Since both *homo-* and *hetero*-association are treated, elementary equilibrium constants in two-dimensional space (i, j) are attenuated by a factor of $1/ij$ in each step.

One more term to the entropy change, which is particularly significant for aqueous and other H-bonded systems, must taken into consideration. It has to describe a disorder in orientation and partially in proton position (because of possible jumping along H-bonds) in the network of strongly directionally depending intermolecular interactions. Hence, it can be called an orientational contribution (ΔS_{orient}) and can be approximately evaluated by an additional parameter of arbitrary directionality (ω) as

$$\Delta S_{\text{orient}} = R \log \frac{1}{\omega^{i+j}} \qquad (10)$$

This new parameter may be understood as an arbitrary number of molecular orientations. Namely, it is supposed that the highly directional potential present in hydrogen bonded mixtures acts through a small solid angle Ω. Hence, every molecule has $\omega = 4\pi/\Omega$ possible orientations, and the large value of ω corresponds to an extremely directional interaction. Since Ω is an arbitrary quantity, the parameter ω is also of the same type. It means that ω has to be adjusted for each system, although some kinds of "universality", i.e., close values are expected for solutions with similar types of molecular interactions. In the present work an experimental temperature slope of ^{1}H NMR shift of H_2O signal ($\Delta\delta/\Delta T$) in homogeneous (one-phase)

solution was used as the criterion adjusting its value (details below).

It is easily seen that the expression of the total entropy change

$$\Delta S = \Delta S_{\text{permut}} + \Delta S_{\text{stack}} + \Delta S_{\text{orient}} = -R \log(i!j!) - R \log(\omega^{i+j}) \quad (11)$$

radically simplifies the calculation of determinants of graph vertices (4) by replacing

$$\binom{i+j}{i}K_{ij} \rightarrow \frac{1}{i!j!\omega^{i+j}} \exp(-\Delta H_{ij}/RT) \qquad (12)$$

The simplification means that now the determinants D_{ij} can be constructed easier because a large data set (experimental and theoretical values) of energies (ΔH) of various molecular interactions in aqueous and other solutions is available in literature. In very peculiar cases they can be evaluated using well-developed methods of quantum chemistry.

Besides thermodynamics, the knowledge of certain *micro*-parameters (depending on what is modeled) of aggregates A_iB_j (δ_{ij}) is necessary. Since NMR chemical shift is to be modeled, various molecular structures of "free" molecules and H-bond complexes were studied and magnetic screening tensors were calculated by density functional theory (DFT). Details of the calculation are given in Chapter III.

The modeling of NMR shifts in the chain of eqs 3−12 has been realized using the Maple programming system.[23] Its results are presented in Chapter IV.

III. DFT Calculations of Magnetic Screenings and NMR Shifts

As mentioned above, an evaluation of ^{1}H NMR shifts in different contacting situations (A···A, A···B, etc.), was based on the quantum chemical density functional theory (DFT) calculations of magnetic shielding tensor of various molecular structures. The applied approach was checked in various cases earlier[24,25] and found to be adequate for this purpose. It produces an excellent coincidence of calculated and experimentally measured ^{1}H NMR shift for nuclei in very strong H-bond systems, e.g., bridge proton in pyridine-N-oxide···HCl complex,[24] as well as for rather "inert" groups, e.g., $-CH_3$ protons of acetonitrile.[25]

The full geometry optimization in the ground state was performed using Becke's three parameter hybrid method and the Lee−Yang−Parr functional (B3LYP)[26−28] combined with 6-311++G** basis set.[29,30] The Gaussian 03 program package[31] was used for all our calculations. Magnetic shielding tensors (σ) have been calculated using Perdew and Wang's 1991 gradient-corrected correlation functional (B3PW91), the modified hybrid functional of Perdew, Burke, and Ernzerhof (PBE1PBE)[32−34] and the gauge-including atomic orbital (GIAO) approach.[35] To take into account the solvent effect, we applied the polarized continuum model (PCM) of Tomasi and co-workers.[36,37] The ^{1}H chemical shifts of the investigated molecular structures (water clusters and pyridine/water H-bond complexes) were transformed to the δ-scale as the difference between the calculated isotropic magnetic shielding (σ_{iso}) and that of the tetramethylsilane (TMS) as reference molecule.[24,25]

IV. Results and Discussion

Water (component A)/pyridine (component B) solution has been chosen as the model system for the following reasons. A

broad variety of phase transitions are reported for aqueous solutions of derivatives of pyridine. Binary systems of water/ pyridine and water/one-methyl-substituted pyridine are completely miscible, but those of water/two-methyl-substituted pyridine and /one-ethyl-substituted pyridine exhibit very fascinating closed-loop phase diagrams.[38] Phase separations in completely miscible water/pyridine mixtures can be induced by the introduction of an ionic subsystem.[5,39] Also quantum chemistry calculations on these systems (water clusters, water/ derivatives of pyridine complexes) are well advanced.[40–44] These results can be useful for comparative purposes.

IV.A. Magnetic Screening Properties. Table 1 displays all calculated molecular aggregates, values of the isotropic part of magnetic shielding tensor and ^{1}H NMR chemical shift $\langle\delta_{ij}\rangle$, where $\langle...\rangle$ denotes an averaging over all "mobile" (i.e., enrolled into fast exchange processes, eq 1) protons in corresponding structures. The existence of optimized water structures, i.e., near-linear hydrogen-bonded dimers, cyclic trimers, and cyclic tetramers (Table 1), is supported by measurements of vibration– rotation tunneling spectra and FT-IR spectra of water in low-temperature matrix isolation.[45–48] It is obvious that a segregation of pure dimer, trimer, etc. in liquid water is not feasible due to dynamic averaging (eq 2), and thus, NMR shifts of these structures have never been evaluated experimentally. Consequently, a comparison of calculated NMR shift values with experimental data is possible for bulk (i.e.. $\delta(x_A = 1)$) and "monomeric" water ($\delta(x_A \rightarrow 0)$) only. Experimental data are well-known: 4.72 ppm in the bulk water,[49] and these values are spread at an infinite dilution in various solvents over 0.4– 1.4 ppm depending on solvent.[50] A sigmoidal-like dependence of calculated chemical shift of water aggregates $\langle\delta_{i0}\rangle$ as a function of $1/i$ is shown in Figure 2. The calculation of monomeric water using two different DFT functionals (Chapter III) gives the values of its chemical shift ca. 0.1 ppm in vacuo and between 0.6 and 1.54 ppm in water as solvent. It is unreasonable to expect a better agreement with experimental values (e.g., 0.4 ppm in benzene, 1.2 ppm in CCl₄, 1.4 ppm in C_6H_{12}[50]) as no additional corrections due to the magnetic susceptibility of different solvent effects were made. Note the susceptibility contribution to chemical shift can be rather large ($\sim$1–1.5 ppm), but it is only weakly temperature dependent.[51] Hence, it can be neglected in modeling the thermal behavior of the NMR shift.

^{1}H NMR shifts of $(H_2O)_i$ increase with increasing aggregation number i, and already in the pentamer and hexamer they top a value for bulk water (Figure 2). Therefore, these structures are considered to be dominant in liquid water.[52] In addition, a tetrahedrally coordinated pentamer (structure V, Table 1) was studied in the present work in order to evaluate the chemical shift of water in the limiting aggregation case of $i \rightarrow \infty$. This structure was optimized keeping tetrahedral symmetry of oxygen atoms frozen and including reaction field of water via the PCM. The ^{1}H NMR shift of 5.5 ppm was obtained by averaging chemical shifts of "internal" protons (circled protons in V, Table 1). The obtained δ(^{1}H) value, being in good agreement with the gas-to-liquid shift of 5.8 ± 0.1 ppm,[53] limits the whole extent of chemical shifts of the liquid water. It lies between those of bulk water (4.72 ppm) and ice ($\sim$8 ppm).[53]

Surprisingly, despite quite simple model treatment, a satisfactory agreement with experimental values was obtained. It looks like an extra support to one recipe of calculations that is widely used in quantum chemistry, and that leads to good results. Namely the short-range interactions, usually presented in

condensed phases, can be effectively handled by a "supermolecule" model (i.e., a solute molecule surrounded by several solvent molecules (in the present case, all water) calculations. Furthermore the inclusion of solvent reaction field provides an effective description of long-range electrostatic interactions.[54] Nevertheless, note that the averaging even over two protons in the "central" water molecule in the tetrahedral pentamer does not reproduce the value of ^{1}H NMR shift in ice\ completely (6.2 ppm in comparison with experimental $\sim$8 ppm[53]). Possibly, the PCM does not describe the ordered crystalline field satisfactory, or this pentamer structure is still too small to describe major short-range interactions in ice adequately.

The calculated $\langle\delta_{ij}\rangle$ using PBE1PBE functional seems to be more acceptable. In addition, an excellent agreement between PBE1PBE calculations and experimental data can be noted for ^{13}C and [17]O magnetic screenings in many other molecular systems, and in particular, in studying hydrogen bonding and proton-transfer processes.[55]

IV.B. Association Energies. In the current work, we did not concentrate ourselves on the precise evaluation of binding energies of various water–water and water–pyridine structures. On the one hand, these data are rather well-known from numerous and thorough works devoted mainly to the equilibrium structures and energy problems. A broad set of quantum chemistry tools and sophisticated refinements were applied to this purpose (refs 40–44, 52, and references cited therein). On the other hand, there is no need to know these energies very precisely. For the attainment of the goal stated in the introduction, i.e., to determine physical margins for the evaluation of critical indices, it is necessary to span the modeling over a broad range of interaction energies that are introduced as model input parameters. Summarizing our data and the literature data on molecular association energies, we chose the following energy values: (1) ΔE_{AA} (association energy per one bond (H-bond) in water clusters) = 3–5 kcal/mol; (2) ΔE_{AB} (H-bond energy in water/pyridine complex) = 6–8 kcal/mol; (3) ΔE_B ("stacking" energy of B-molecule, i.e., pyridine binding energy via other types of interaction that differ from H-bond) = 0–4 kcal/ mol. This range was chosen using data from refs 42, 43, 56, 57.

IV.C. Enthalpies and Chemical Shifts. It is most convenient to split the averaging of chemical shift (3) into two stages: an internal averaging within each cluster and that over the whole statistical ensemble. The cluster "internally" averaged chemical shift $(\langle\delta_{ij}\rangle = \Sigma\delta_{ij}/(in_A + jn_B)$, where n_A and n_B are the numbers of mobile protons in A and B molecules respectively) are already given in Table 1. In this case, the Mason's rule (eq 3) for mobile protons in an A/B solution has to be modified introducing the weight factors $in_A + jn_B$:

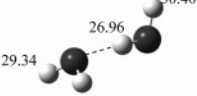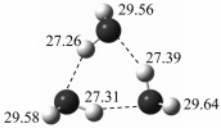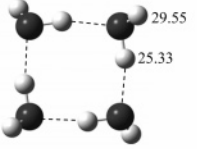$$\langle\delta\rangle = \sum_{i,j} D_{ij}(in_A + jn_B)\langle\delta_{ij}\rangle / \sum_{i,j} (in_A + jn_B)D_{ij}$$
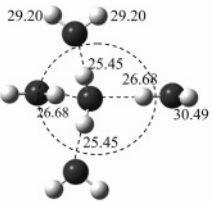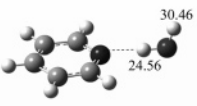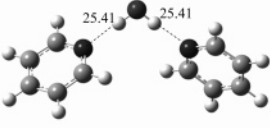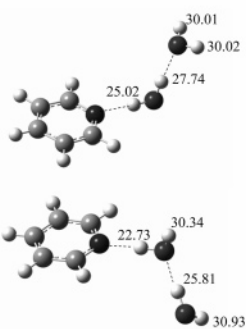
which, after the balance eqs 6 are taken into account, becomes

$$\langle\delta\rangle = \sum_{i,j} D_{ij}(in_A + jn_B)\langle\delta_{ij}\rangle / (n_A x_A + n_B x_B) \qquad (13)$$

Since two mobile protons are donated by a water molecule and not one from pyridine, the values $n_A = 2$ and $n_B = 0$ have to be inserted into eq 13.

The ΔH_{ij} and δ_{ij} sets were constructed taking into account specific details of molecular interactions in the system under consideration. Calculated ^{1}H NMR shift values (Table 1)

NMR Shifts by Statistical Thermodynamics and DFT Calculations

J. Phys. Chem. B, Vol. 111, No. 10, 2007 **2527**

TABLE 1: Calculated Structures, Isotropic Parts of ^1H Shielding Tensors, and ^1H NMR Chemical Shift $\langle\delta\rangle$ Averaged over All Protons in Structure (all in ppm). Chemical Shifts Were Recalculated with Respect to TMS Molecules as NMR Standard Using $\sigma_{iso}(^1H, TMS) = 31.6$ ppm (in Water)

		$\langle\delta\rangle$
I.	Non-bonded water	
	30.06	1.54
II.	Dimer	
	30.40	
	26.96	
	29.34	2.59
III.	Trimer	
	29.56	
	27.26	
	27.39	
	27.31	
	29.58	29.64	3.14
IV.	Tetramer	
	29.55	
	25.33	4.16
V.	Pentamer [a]	
	29.20	29.20	
	25.45	
	26.68	
	26.68	30.49	
	25.45	5.5
VI.	Water - pyridine 1:1 complex	
	30.46	
	24.56	4.25
VII.	Water - pyridine 1:2 complex	
	25.41	25.41	6.19
VIII, IX.	Water - pyridine 2:1 complexes [b]	
	30.01	
	30.02	
	25.02	27.74	3.40
	30.34	
	22.73	
	25.81	
	30.93	4.15

[a] Tetrahedral symmetry for "central" oxygen was frozen. [b] Two stables structures were found having -400.818290 and -400.821359 a.u. energies, respectively.
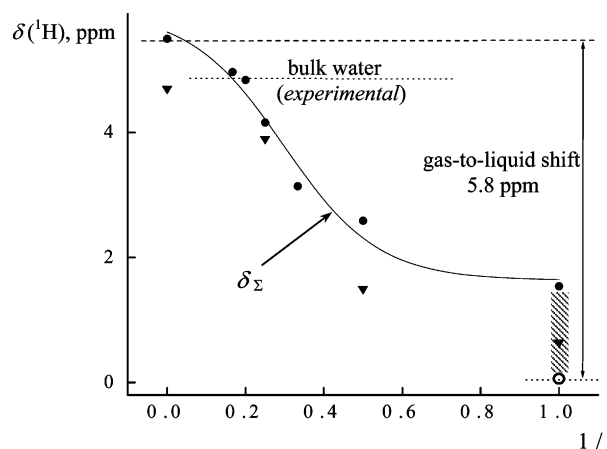

Figure 2. ^1H NMR shift of structures $(H_2O)_i$ at increasing number of aggregation (i) calculated using B3PW91 ($\blacktriangledown$) and PBE1PBE ($\bullet$) functionals in water solvent field. Presentation in $1/i$ as variable was chosen for convenience to put the limiting case $i \rightarrow \infty$ to the graph. Experimental values of water monomer in various solvents (taken from ref 50) are shown by dashed area. Calculated monomer shift in vacuo is shown by open circle, pentamer and hexamer shifts are taken from ref 52, and the gas-to-liquid shift from ref 53. The sigmoidal fit Boltzman function $\delta_\Sigma = f(1/i)$ on PBE1PBE data is shown by solid line (see Appendix 1).

TABLE 2: The Basic Set of Parameters Used in Simulation of ^1H NMR Shifts

energies (cal/mol):
$\Delta H_{00} = \Delta H_{10} = \Delta H_{01} = 0;$
$\Delta H_{11} = 6530$ (DFT value for water/pyridine complex[42]);
$\Delta H_{20} = 3760$ (water dimerization energy, present work);
$\Delta E_{AA} = 4000; \Delta E_{AB} = 7000; \Delta E_B = 0$
(an arbitrary choice, but these values will be varied at the simulation in the margins discussed above).

chemical shifts (ppm):
$\delta_{00} = \delta_{01} = 0;$
$\delta_{10} = 1.54$ (water monomer);
$\delta_{20} = 2.59$ (water dimer);
$\delta_{11} = 4.25$ (water$\cdots$pyridine 1:1 complex);
$\delta_{30} = 3.14$ (water trimer);
$\delta_{21} = 4.15$ (water$\cdots$pyridine 2:1 complex);
$\delta_{12} = 6.19$ (water$\cdots$pyridine 1:2 complex, all from Table 1);

critical parameters:
$\alpha = 0.110; \beta = 0.3255; \Delta_s = 0.51; T_U = 503.85$ K; $T_L = 307.15$ K;
$x_U = 0.605; x_L = 0.688$ (both in mass fraction);
$B_0 = 1.064; B_1 = -0.46; B_a = 1.07; d_1 = -0.130$ (all from ref 20).
note. because of averaging (13) requires composition in mole fractions, the concentrations were converted into mole fractions (Figure 3), and the amplitudes were recalculated.

orientational-positional disorder:
$\omega = 1$, i.e., $\Delta S_{orient} = 0$. this value also was varied at the simulation.

together with sigmoidal fitted ones $\delta_\Sigma(i)$ (Figure 2 and Appendix 1) were used as the basic quantities constructing the whole set of δ_{ij}. First we "decorate" the graph of chemical equilibria (Figure 1) by segregation of "short-range" structures, i.e., three-particle associates ($i + j \leq 3$) and setting to them special values of δ_{ij}. They are given in Table 2. And one more useful parameter is introduced, $\delta_{AB} = 7.04$ ppm, i.e., the chemical shift of proton in the H-bond N$\cdots$H$-$O (a bridge proton in structure VI, Table 1).

For larger structures ($i + j > 3$), the following approach constructing ΔH_{ij} and δ_{ij} is applied:

$$\Delta H_{ij} = \begin{cases} (i-j)\Delta E_{AA} + j\Delta E_{AB}, & \text{if } i \geq j \\ i\Delta E_{AB} + (j-i)\Delta E_{B}, & \text{otherwise} \end{cases} \text{ and}$$

$$\delta_{ij} = \begin{cases} \delta_{\Sigma}(i-j) + j\delta_{AB}, & \text{if } i \geq j \\ \delta_{\Sigma}(i) + i\delta_{AB}, & \text{otherwise} \end{cases} \quad (14)$$

In other words, replacing of A(water) molecule by B(pyridine) leads to a formation of much stronger H-bonding A⋯B, if water molecules are present in the A_iB_j aggregate in excess. Otherwise the attachment of B goes only via stacking interaction that is characterized by the parameter ΔE_B.

ΔE_{AA} and E_{AB} have been introduced for higher flexibility of the modeling mainly. Roughly speaking $\Delta H_{20} \approx \Delta E_{AA}$ and $\Delta H_{11} \approx \Delta E_{AB}$. However ΔH_{20} and ΔH_{11} are much better determined by DFT calculations of water dimer and 1:1 water/pyridine complex. The contributions of these structures into averaging (eq 13) are very significant. Therefore, these values were kept "frozen" in some sets of the model input parameters (Tables 2 and 3), whereas the ΔE_{AA} and ΔE_{AB} used evaluating ΔH_{ij} for higher aggregates (eq 14) were varied over the given energy ranges.

Of course, these "Lego"-like constructions (eq 14) are far from being precise, but this blemish is likely compensated in the simplest way to include all A_iB_j aggregates into the averaging procedure (eq 13), even those of the limiting case $i, j \rightarrow \infty$. Moreover, intrinsic details of structure and interactions in small clusters are less important near the critical region then is widely believed

A sort of "coherency" in variation of ΔH_{ij} and δ_{ij} in (14) at running indices (i, j) has been chosen, exploiting the idea of almost linear response of the system of type "interaction strength" ⟷ "change (shift) of parameter of bonded with respect to nonbonded species", analogous to the well-known correlation $\Delta H \sim \Delta\nu$, often used in IR spectroscopy of hydrogen bonding.[43,58]

To take into account an orientational entropy contribution (eq 10) the parameter ω (an arbitrary number of molecular orientations) has to be included into the modeling. It needs some adjustment, and as a criterion for this procedure, the best reproduction of experimental dependencies of certain physical properties on temperature or composition may be used. For example, in the case of closed-loop coexistence curves analysis,[59,60] the closed-loop widths were used for this purpose. Since temperature dependencies of ^{1}H NMR shift in aqueous solution are going to be simulated in the present work, the value $\omega \approx 24$ was found when trying to reproduce the experimental temperature slopes of ^{1}H NMR shift of H_2O signal in one-phase region, $(\Delta\delta/\Delta T) = -0.013 \pm 0.001$ ppm/K. Note the same value of ω was found as optimal in ref 61, where it has been adjusted trying to reproduce the experimental temperature slopes $(\Delta\delta/\Delta T)$ of ^{1}H and ^{17}O NMR shifts in the neat water. One more value, $\omega = 12$, i.e., the number of nearest neighbors in fcc quasi-lattice, was used in simulation for comparative purposes.

IV.D. Modeling Results. In the case where a system possesses a closed-loop phase diagram characterized by both a lower critical solution point (LCSP) and an upper one (UCSP), the expression for concentration along the phase coexistence boundary (7) becomes the following:[20]

$$x^{\pm} = x_L \pm B_0|\tau_{UL}|^{\beta}[1 + B_1|\tau_{UL}|^{\Delta s}] + B_a|\tau_{UL}|^{1-\alpha} +$$
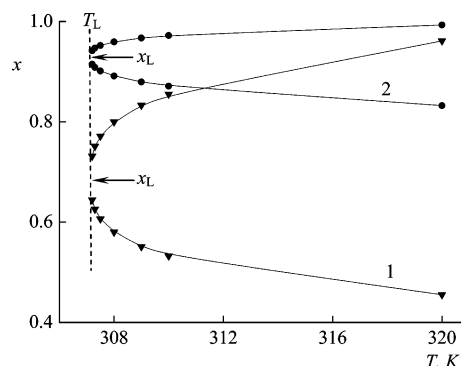$$d_1(T - T_L)/T_L \quad (15)$$

Figure 3. The phase diagrams of H_2O/2,6-lutidine solution close to the lower critical solution point ($T_L = 307.15$ K) in the cases concentration of H_2O (x) are given in mass (1, eq 15) or mole (2) fractions. The critical concentrations are $x_L = 0.688$ mass fraction and 0.929 mole fraction respectively. Concentrations used in the NMR shifts modeling are marked as points on the diagram.

where superscripts ($\pm$) correspond to the sign $\pm$ in the equation, the critical parameters are T_U, T_L are the temperatures of UCSP and LCSP, x_U, x_L are the corresponding concentrations, B_0, B_1, B_a are the amplitudes, and α, β, Δ_s are the indices, respectively, $\tau_{UL} = (T - T_U)(T - T_L)/T_U T_L$; $d_1 = (x_U - x_L)/(T_U - T_L)$. We try to use parameters of the water/2,6-lutidine system, because very precise NMR experimental data are available for this solution.[11] The values of these parameters, taken from ref 20, are presented in Table 2. The phase diagram in the vicinity of T_L is shown in Figure 3.

The most precise experimental data are usually obtained in a region close to the LCSP. Difficulties due to chemical stability of compounds and temperature stabilization, which are quite often met close to the UCSP, make measurements in the vicinity of T_U less reliable. Therefore, the modeling was carried out in the temperature range of 307.15−320K. Temperature dependencies of chemical shifts in coexisting phases (δ^+ and δ^- correspond to x^+ and x^- respectively, eq 15) and "critical" chemical shift, i.e., $\delta_C = \delta(x_L, T_L)$, have been simulated using various sets of model parameters (Tables 2 and 3). Later on these quantities have been used in constructing a so-called "chemical shift order parameter"

$$\Delta\delta = |\delta^+ - \delta^-| \quad (16)$$

and a "diameter of chemical shift"

$$\phi\delta = |(\delta^+ + \delta^-)/2 - \delta_C| \quad (17)$$

which have been processed in each case using linear regression analysis of $\Delta\delta \sim |T - T_L|$ and $\phi\delta \sim |T - T_L|$ in the log−log plot. The whole scheme of modeling (Scheme 1) is given in Appendix 2.

Some typical results of this modeling are presented in Figures 4 and 5. Corresponding slope values are collected in Table 3. It is easy to see that the critical index β can be evaluated from the slope of $\Delta\delta = f(T - T_L)$ with high precision at any meaningful set of model input parameters. It is most important that this slope is practically independent of energies of intermolecular interactions (Table 3). It makes this parameter a universal one for a broad variety of critical systems having rather different energies and network of molecular association via *homo-* and *hetero-* H-bonding, stacking, etc. Moreover, the $\Delta\delta$ slope value very precisely (± 0.01) follows any perturbation of input values of β (0.3−0.4), and thus it can be applied studying fine peculiarities of critical behavior, e.g., solvophobic vs ionic critical regimes.
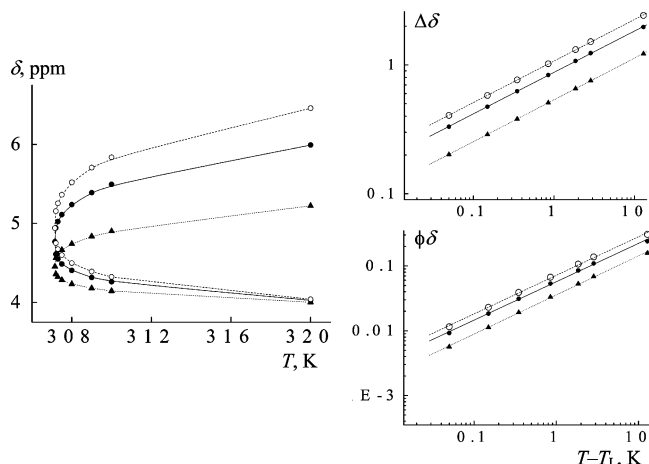
Figure 4. Temperature dependencies of ^{1}H NMR shifts of water (δ), order parameter ($\Delta\delta$) and diameter ($\phi\delta$) simulated using the "basic" set of input parameters for water/2,6-lutidine solution (●, see Table 2) and perturbing the energy of A···B interaction, i.e., all parameters are the same as in the "basic" set, only ΔE_{AB} changes $\Delta E_{AB} = 6000$ (▲) and 8000 cal/mol (○) respectively. $\Delta\delta$ and $\phi\delta$ slope values are given in Table 3.
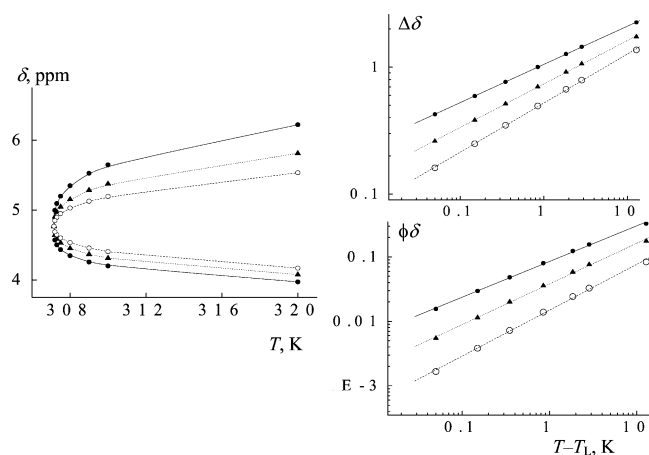

Figure 5. Temperature dependencies of ^{1}H NMR shifts of water (δ), order parameter ($\Delta\delta$) and diameter ($\phi\delta$) simulated using the "basic" set of input parameters for water/2,6-lutidine solution (Table 2) and perturbing the critical index β value only: $\beta = 0.3$ (●), 0.35 (▲), and 0.4 (○), respectively. $\Delta\delta$ and $\phi\delta$ slope values are given in Table 3.

TABLE 3: The Slopes of ^{1}H NMR Shift Order Parameter and Diameter Obtained by Linear Regression Analysis of $\Delta\delta$ and $\phi\delta$ *vs* $T - T_L$ in Log–log Plot[a]

perturbation of basic set	slope of $\Delta\delta$	slope of $\phi\delta$
no perturbation (parameter values in Table 2)	0.319 ± 0.002	0.580 ± 0.013
$\Delta E_{AA} = 3000$	0.321 ± 0.004	0.539 ± 0.022
$= 5000$	0.319 ± 0.002	0.583 ± 0.012
$\Delta E_{AB} = 6000$	0.321 ± 0.001	0.587 ± 0.011
$= 8000$	0.322 ± 0.002	0.591 ± 0.010
$\Delta E_B = 2000$	0.319 ± 0.002	0.579 ± 0.013
$= 4000$	0.313 ± 0.003	0.540 ± 0.015
$\Delta H_{20} = 2000$	0.319 ± 0.002	0.582 ± 0.012
$= 6000$	0.319 ± 0.002	0.552 ± 0.019
$\Delta H_{11} = 4000$	0.323 ± 0.001	0.597 ± 0.009
$= 8000$	0.323 ± 0.002	0.600 ± 0.007
$\alpha = 0$	0.323 ± 0.001	0.604 ± 0.007
$= 0.2$	0.314 ± 0.005	0.552 ± 0.016
$\beta = 0.3$	0.298 ± 0.002	0.543 ± 0.011
$= 0.35$	0.341 ± 0.003	0.616 ± 0.014
$= 0.4$	0.386 ± 0.004	0.687 ± 0.018
$\omega = 12$	0.318 ± 0.003	0.575 ± 0.014
$= 24$	0.316 ± 0.003	0.563 ± 0.017

[a] Chemical shifts were simulated using the basic set of parameters for water/2,6-lutidine solution (Table 2) and using perturbed values of energies of some interactions (all in cal/mol), critical indices and orientational disorder.
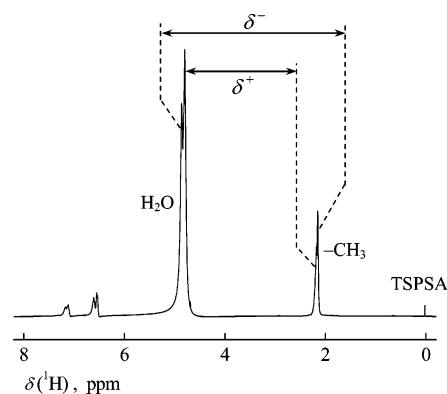

Figure 6. ^{1}H NMR spectrum of H$_2$O/2,6-lutidine solution in two-phase region. The shifts δ^+ and δ^- of split signals (see zoom in Figure 7) used in "order parameter" and "diameter" calculations (eqs 16, 17) correspond to the water-rich and 2,6-lutidine-rich phases. The solution of TSPSA[49] in D$_2$O in capillary insert was used as a reference signal.

A situation with the slope of "diameter" of chemical shifts is much more complicated. A priori looking into phase coexistence boundary eq 15 it was expected that the diameter close to T_L should obey an asymptotic $\phi\delta \sim |T - T_L|^{1-\alpha}$. But during the modeling of chemical shifts it has been found that thermal behavior of $\phi\delta$ depends as well on input β as on input α values (Table 3). The obtained $\phi\delta$ slopes (0.58–0.71) are rather far from the expected $1 - \alpha$, but very close to 2β values.

IV.E. Comparison with Experiment. The doubling of NMR signals of various nuclei crossing the border between homogeneous and separated phases was observed in many cases.[10–14] The most precise experiment has been carried out on D$_2$O/2,6-lutidine solution.[11] A specially constructed NMR probe head allowed us to achieve the temperature stabilization accuracy within $\pm$ 0.005K. The value of the critical index β, obtained from the split ^{2}H NMR signal of D$_2$O temperature evolution, i.e., from $\Delta\delta$ vs $T - T_L$, $\beta = 0.336 \pm 0.030$, is in perfect agreement with data of the present simulation. Unfortunately no place for additional tube or capillary insert for external reference signal was projected in that NMR probe head. Thus,

because of no reference peak (single or doubled D$_2$O signal only), the diameter of chemical shift was not investigated in this system.

A new experiment on H$_2$O/2,6-lutidine system was performed using a standard NMR probe head that allows temperature precision within ± 0.5 K. It enabled us to investigate the temperature behavior as for the 'order parameter' as well as for the diameter of chemical shifts. H$_2$O/2,6-lutidine solution of 0.937 mole fraction of H$_2$O, i.e., the value between those found in literature,[11,20] was prepared. The onset of NMR signal splitting was observed at 306.0 ± 0.5 K, and this temperature was recognized as the lower critical solution point T_L. A typical experimental spectrum in the two-phase region is shown in Figure 6. The thermal equilibration influences on the NMR signal shapes and chemical shifts (Figure 7). This influence is the more significant the closer to critical point experiments run. In the vicinity of the phase separation point ($T - T_L \approx 0.5$ K) it can take ~30 min till it has no practical affect on chemical shifts. Also note, that the whole effect of phase separation on chemical shifts is not large, viz., the split signals are changed at $T - T_L = 10$ K by ~0.3 ppm only. It means a very high
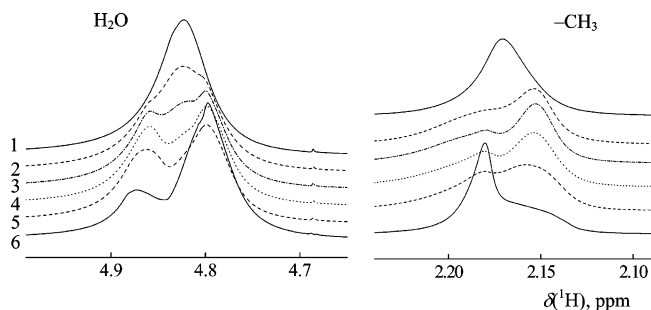
Figure 7. ^{1}H NMR monitoring of the thermal equilibration process in the H$_2$O/2,6-lutidine solution close to the phase separation point: (1) $T = 306.5$ K is just set up and after; (2) 1 min; (3) 2 min; (3) 3 min; (4) 5 min; (5) 10 min; (6) 30 min.
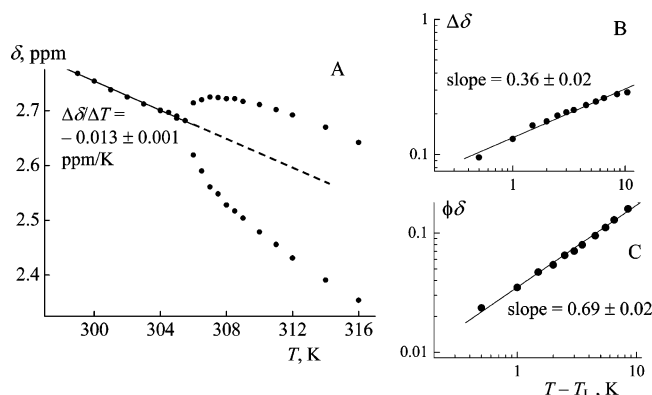

Figure 8. Experimental temperature dependencies of ^{1}H NMR shift of H$_2$O protons with respect to $-$CH$_3$ signal (an internal reference) in the H$_2$O/2,6-lutidine solution of critical composition in the one- and two-phase regions (Part A). Results of the linear regression analysis of the order parameter ($\Delta\delta$) and the diameter ($\phi\delta$) in log$-$log scale are presented in Parts B and C, respectively. The value of $\Delta\delta/\Delta T$ in the homogeneous (one-phase) mixture has been used as criterion adjusting the parameter of arbitrary directionality (ω) in eq 10 (see text).

precision in the determination of chemical shifts is desirable during this study. Even the influence of changing magnetic susceptibility may fatally distort experimental data. Therefore the NMR shifts of H$_2$O protons have been measured with respect to the signal of $-$CH$_3$ groups of 2,6-lutidine molecules, i.e., with respect to an internal standard. Temperature dependencies of the ^{1}H NMR shifts, the "order parameter", and the diameter are shown in Figure 8. The obtained values of slopes of the order parameter and the diameter are in perfect agreement with results of the present modeling. The value of $\beta = 0.36 \pm 0.02$ for H$_2$O/2,6-lutidine solution (Figure 8B) is in the margin of error the same as estimated for D$_2$O/2,6-lutidine.[11] The $\phi\delta$ slope 0.69 ± 0.02 (Figure 8C) is experimentally determined for the first time. It is extremely close to the 2β value as predicted by the simulation above. Note the diameter calculation can be distorted by the linear temperature dependence of chemical shifts. As it was already mentioned, the slope $\Delta\delta/\Delta T = -0.013 \pm 0.001$ ppm/K was evaluated in the homogeneous region. However the replacing of the fixed critical chemical shift $\delta_C = \delta(x_L, T_L)$ value in (17) by a linear one as result of prolongation of $\delta(T)$ from one- to two-phase region (the dashed line in Figure 8A) leads not toward a "desirable" $1 - \alpha \approx 0.89$, but even toward lower values of diameter slope (0.60 ± 0.05).

It is suggested that the term in the diameter of coexistence curves containing $|T - T_C|^{2\beta}$ arises from a "wrong" choice of composition variables.[62] For this reason, we have chosen acetic anhydride/*n*-heptane and acetic anhydride/cyclohexane solutions for additional NMR experiments as systems having
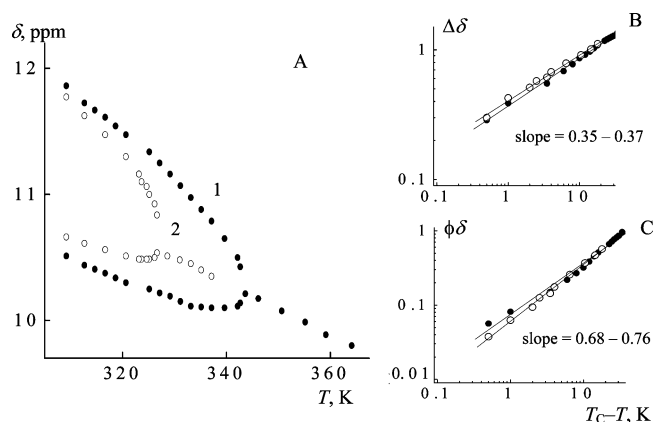

Figure 9. Experimental temperature dependencies of ^{1}H NMR shift of acetic acid (as a molecular probe) in acetic anhydride/*n*-heptane (1) and acetic anhydride/cyclohexane (2) solutions in one- and two-phase regions (Part A). Results of the linear regression analysis of the order parameter ($\Delta\delta$) and the diameter ($\phi\delta$) in log$-$log scale are presented in Parts B and C, respectively.

rather "symmetric" coexistence curves characterized by critical compositions in mole fraction very close to 0.5 (0.47 and 0.575 respectively). Experimental results on temperature dependencies of ^{1}H NMR shift in acetic anhydride/*n*-heptane (1) and acetic anhydride/cyclohexane (2) solutions in one- and two-phase regions using a standard NMR probe head are presented in Figure 9A. Note a very small amount of acetic acid (≥ 0.005 mole fraction) always appears in these samples because of the reaction of acetic anhydride with moisture. Hence molecules of acetic acid, because of extremely high sensitivity of the NMR signals of the $-$COOH proton on temperature and composition, were "useful" to be exploited in these experiments as a molecular probe. The effect of phase separation on $-$COOH chemical shifts is much larger (the split of $\sim$1 ppm at $T_C - T = 10$ K), and therefore, ^{1}H NMR shifts have been measured with respect to an external standard of HMDS[49] in capillary insert.

Despite limited accuracy of temperature stabilization (± 0.5 K), the obtained values of β in the range of 0.35$-$0.37 (Figure 9B) are typical for systems with solvophobic criticality, and they are in good agreement with results of the present modeling. And again, the $\phi\delta$ slope values (0.68$-$0.76, Figure 9C) are close to 2β ones as predicted by the simulation above. The last result, common for all solutions studied, is in certain cohesion with the new concept of "complete scaling" formulated in ref 63 and examined experimentally in ref 64. It seems that the present finding can be considered as a certain additional experimental support to this concept.

V. Concluding Remarks

The modeling of NMR shifts has shown that the critical index β can be evaluated with a high precision from the slope of chemical shift order parameter $\Delta\delta = f(T - T_L)$. The correct value of β is reproduced at any more or less realistic set of model input parameters (energies of interactions, critical data, etc). Hence, this technique can be considered as a convenient and powerful tool studying fine peculiarities of critical behavior, e.g., solvophobic vs ionic critical regimes. Thermal behavior of diameter of chemical shifts seems to be very important in the light of the concept of complete scaling. It inspires further experimental NMR studies extending the choice of critical systems of different degree of asymmetry.

NMR Shifts by Statistical Thermodynamics and DFT Calculations

J. Phys. Chem. B, Vol. 111, No. 10, 2007 **2531**

project "Structure and Phase Transitions in Ionic Solutions". We thank the Danish Center for Scientific Computing (Copenhagen, Denmark) for the use of computational facilities and the Gaussian 03 program package. We are grateful to Professor Z. Gdaniec (Institute of Bioorganic Chemistry, Poznan, Poland) for assistance during NMR experiments, to Professor M. A. Anisimov for stimulating discussions and comments, and also to Professor J. V. Sengers (both University of Maryland) for sending us their latest results on this topic.

Appendix 1

A sigmoidal curve $y = f(x)$ fitting using the Boltzmann 4-parameters equation

$$y = \frac{A_1 - A_2}{1 + e^{(x-x_0)/dx}} + A_2$$

was arbitrary applied processing results of DFT calculations of ^{1}H NMR shifts $\langle \delta_{i0} \rangle = f(1/i)$ presented in Figure 2. This procedure is enrolled in the Microcal Origin program package.[65] Fit parameters values were obtained: $\chi^2 = 0.0918$; $R^2 = 0.9779$; $A_1 = 5.9372$; $A_2 = 1.63581$; $x_0 = 0.29835$; and $dx = 0.11983.x$

Appendix 2

SCHEME 1: General Scheme of Modeling
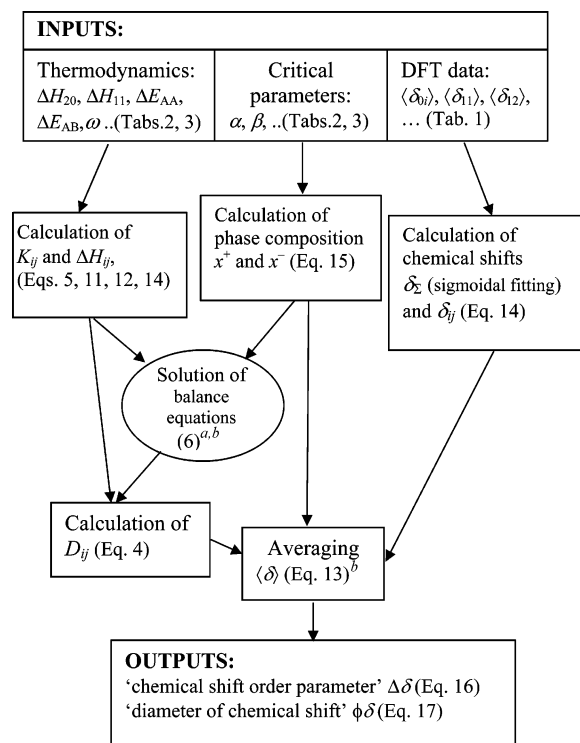
[a] Precision of solution of 10^{-6} was set up. [b] Summing for $i,j = 0$ until $N = 20$ was found to be optimal.

References and Notes

(1) Anisimov, M. A. *Critical Phenomena in Liquids and Liquid Crystals*; Gordon and Breach Science Publishers: New York, 1991.

(2) *New Approaches to Problems in Liquid State Theory*; Caccamo, C.; Hansen, J. P.; Stell, G., Eds.; NATO Advanced Study Institutes, Ser. C, V. 529, Kluwer: Dordrecht, 1999.

(3) Gutkowski, K.; Anisimov, M. A.; Sengers, J. V. *J. Chem. Phys.* **2001**, *114*, 3133-3146.

(4) Narayanan, T.; Parfulla, B. V.; Kumar, A.; Gopal, E. S. R. *Ber. Bunsen–Ges.* **1991**, *95*, 12-14.

(5) Narayanan, T.; Kumar, A.; Venkatachalam, S.; Jacob, J.; Parfulla, B. V. *J. Chem. Phys.* **1995**, *102*, 9653-9658.

(6) Kostko, A. F.; Anisimov, M. A.; Sengers, J. V. *Phys. Rev. E* **2004**, *70*, 026118-11.

(7) Wagner, M.; Stanga, O.; Schroer, W. *Phys. Chem. Chem. Phys.* **2004**, *6*, 580-589.

(8) Langer, R.; Zundel, G. *J. Chem. Soc. Faraday Trans.* **1995**, *91*, 3831-3838.

(9) Martin, M. L.; Delpuech, J. J.; Martin, G. J. *Practical NMR Spectroscopy*; Wiley-Heyden: London, 1980.

(10) Lacelle, S.; Cau, F.; Tremblay, L. *J. Phys. Chem.* **1991**, *95*, 7071-7078.

(11) Balevicius, V.; Weiden, N.; Weiss, Al. Z. *Naturforsch.* **1992**, *47a*, 583 -587.

(12) Matubayasi, N.; Wakai, C.; Nakahara, M. *J. Chem. Phys.* **1997**, *107*, 9133-9140.

(13) Balevicius, V.; Blinc, R. *Lithuanian J. Phys.* **2001**, *41*, 495-499.

(14) Balevicius, V.; Gdanec, Z.; Fuess, H. *J. Chem. Phys.* **2005**, *123*, 224503-5.

(15) *Studies in Physical and Theortical Chemistry 28. Chemical Applications of Topology and Graph Theory*; King, R. B., Ed.; Elsevier: Amsterdam, 1983.

(16) *Application of Graph Theory in Chemistry*; Zefirov, N. S.; Kuchanov S. I., Eds.; Nauka: Novosibirsk, 1988. (in Russian).

(17) Martin, R. B. *Chem. Rev.* **1996**, *96*, 3043-3064.

(18) Davis, D. B.; Dijmant, L. N.; Veselkov, A. N. *J. Chem. Soc. Faraday Trans.* **1996**, *92*, 383-390.

(19) Hernando Santiago, A. A.; Rozvadovska, A. Q.; Evstigneev, M. P. *Abstracts of 3rd International Conference "Physics of Liquid Matter: Modern Problems"*, Kyiv, Ukraine, May 27−31, 2005; pp 35−37.

(20) Wang, J.; Anisimov, M. A.; Sengers, J. V. Z. *Phys. Chem.* **2005**, *219*, 1273-1297.

(21) Wagner, M.; Stanga, O.; Schroer, W. *Phys. Chem. Chem. Phys.* **2003**, *5*, 1225-1234.

(22) Hernandez, M. P.; Ortega, F.; Rubio, R. G. *J. Chem. Phys.* **2003**, *119*, 4428-4436.

(23) Maple Soft software package, http://www.maplesoft.com.

(24) Balevicius, V.; Aidas, K.; Tamuliene, J.; Fuess, H. *Spectrochim. Acta, Part A* **2005**, *61*, 835−839.

(25) Aidas, K.; Balevicius, V. *J. Mol. Liquids* **2006**, *127*, 134 − 138.

(26) Becke, A. D. *J. Chem. Phys.* **1993**, *98*, 5648-5652.

(27) Parr, R. G.; Yang, W. *Density-Functional Theory of Atoms and Molecules*; Oxford University Press: Oxford, 1989.

(28) Lee, C.; Yang, W.; Parr, R. G. *Phys. Rev. B* **1988**, *41*, 785-789.

(29) Krishnan, R.; Binkley, J. S.; Seeger, R.; Pople, J. A. *J. Chem. Phys.* **1980**, *72*, 650-654.

(30) Clark, T.; Chandrasekhar, J.; Schleyer, P. V. R. *J. Comp. Chem.* **1983**, *4*, 294-301.

(31) Frisch, M. J.; Trucks, G. W.; Schlegel, H. B.; Scuseria, G. E.; Robb, M. A.; Cheeseman, J. R.; Montgomery, J. A., Jr.; Vreven, T.; Kudin, K. N.; Burant, J. C.; Millam, J. M.; Iyengar, S. S.; Tomasi, J.; Barone, V.; Mennucci, B.; Cossi, M.; Scalmani, G.; Rega, N.; Petersson, G. A.; Nakatsuji, H.; Hada, M.; Ehara, M.; Toyota, K.; Fukuda, R.; Hasegawa, J.; Ishida, M.; Nakajima, T.; Honda, Y.; Kitao, O.; Nakai, H.; Klene, M.; Li, X.; Knox, J. E.; Hratchian, H. P.; Cross, J. B.; Bakken, V.; Adamo, C.; Jaramillo, J.; Gomperts, R.; Stratmann, R. E.; Yazyev, O.; Austin, A. J.; Cammi, R.; Pomelli, C.; Ochterski, J. W.; Ayala, P. Y.; Morokuma, K.; Voth, G. A.; Salvador, P.; Dannenberg, J. J.; Zakrzewski, V. G.; Dapprich, S.; Daniels, A. D.; Strain, M. C.; Farkas, O.; Malick, D. K.; Rabuck, A. D.; Raghavachari, K.; Foresman, J. B.; Ortiz, J. V.; Cui, Q.; Baboul, A. G.; Clifford, S.; Cioslowski, J.; Stefanov, B. B.; Liu, G.; Liashenko, A.; Piskorz, P.; Komaromi, I.; Martin, R. L.; Fox, D. J.; Keith, T.; Al-Laham, M. A.; Peng, C. Y.; Nanayakkara, A.; Challacombe, M.; Gill, P. M. W.; Johnson, B.; Chen, W.; Wong, M. W.; Gonzalez, C.; Pople, J. A. *Gaussian 03*, revision C.02; Gaussian, Inc.: Wallingford, CT, 2004.

(32) Perdew, J. P.; Burke, K.; Wang, Y. *Phys. Rev. B* **1996**, *54*, 16533-16539.

(33) Perdew, J. P.; Burke, K.; Ernzerhof, M. *Phys. Rev. Lett.* **1997**, *78*, 1396.

(34) Adamo, C.; Barone, V. *J. Chem. Phys.* **1999**, *110*, 6158-6170.

(35) Hinton, J. F.; Wolinski, K. In *Theoretical Treatments of Hydrogen Bonding*; Hadzi, D., Ed.; John Wiley & Sons: Chichester, 1997; pp 75-95.

(36) Barone, V.; Cossi, M.; Tomasi, J. *J. Comp. Chem.* **1998**, *19*, 404-417.

(37) Cances, E.; Mennucci, B.; Tomasi, J. *J. Chem. Phys.* **1997**, *107*, 3031-3041.

(38) Goldstein, R. E. *J. Chem. Phys.* **1983**, *79*, 4439-4447.

(39) Jacob, J.; Kumar, A.; Anisimov, M. A.; Povodyrev, A. A.; Sengers, J. V. *Phys. Rev. E* **1998**, *58*, 2188-2200.

(40) Clementi, E.; Corongiu, G. In *Theoretical Treatments of Hydrogen Bonding*; Hadzi, D., Ed.; John Wiley & Sons: Chichester, 1997; pp 265-293.

(41) Koeddermann, T.; Schulte, F.; Huelsekopf, M.; Ludwig, R. *Angew. Chem. Int. Ed.* **2003**, *42*, 4904-4908.

(42) Papai, I.; Jancso, G. *J. Phys. Chem. A* **2000**, *104*, 2132-2137.

(43) Schoone, K.; Smets, J.; Ramaekers, R.; Houben, L.; Adamowicz, L.; Maes, G. *J. Mol. Struct.* **2003**, *649*, 61-68.

(44) Sicilia, M. C.; Nino, A.; Munoz-Caro, C. *J. Phys. Chem. A* **2005**, *109*, 8341-8347.

(45) Liu, K.; Cruzan, J. D.; Saykally, R. J. *Science* **1996**, *271*, 929-933.

(46) Cruzan, J. D.; Braly, L. B.; Liu, K.; Brown, M. G.; Loeser, J. G.; Saykally, R. J. *Science* **1996**, *271*, 59-62.

(47) Ceponkus, J.; Nelander, B. *J. Phys. Chem. A* **2004**, *108*, 6499-6502.

(48) Ceponkus, J.; Karlstrom, G.; Nelander, B. *J. Phys. Chem. A* **2005**, *109*, 7859-7864.

(49) *Almanac*; Bruker-Biospin:Rheinstetten, Germany, 2005.

(50) Nakahara, M.; Wakai, C. *Chem. Lett*. **1992**, 809-812.

(51) Modig, K.; Halle, B. *J. Am. Chem. Soc.* **2002**, *124*, 12031-12041.

(52) Borowski, P.; Jaroniec, J.; Janowski, T.; Wolinski, K. *Mol. Phys.* **2003**, *101*, 1413-1421.

(53) Pfrommer, B. G.; Mauri, F.; Loule, S. G. *J. Am. Chem. Soc.* **2000**, *122*, 123-129.

(54) Mennucci, B.; Martinez, J. M.; Tomasi, J. *J. Phys. Chem. A* **2001**, *105*, 7287-7296.

(55) Balevicius, V.; Aidas, K.; Kimtys, L.; Hadzi, D. *Abstracts of XVIth International Conference "Horizons in Hydrogen Bond Research"*, August 29 to September 4, 2005, Roskilde, Denmark; p 63.

(56) A(56) Sinnoknot, M. D.; Sherrill, C. D. *J. Am. Chem. Soc.* **2004**, *126*, 7690 -7697.

(57) Tsuzuki, S.; Honda, K.; Uchimaru, T.; Mikami, M. *J. Am. Chem. Soc.* **2002**, *124*, 104-112.

(58) Iogansen, A. V. In *Hydrogen Bonding*; Sokolov, N. D., Ed.; Nauka: Moscow, 1981; pp 112−155. (in Russian).

(59) Andersen, G. R.; Wheeler, J. C. *J. Chem. Phys.* **1978**, *69*, 2082-2088.

(60) Andersen, G. R.; Wheeler, J. C. *J. Chem. Phys.* **1978**, *69*, 3403-3413.

(61) Balevicius, V.; Aidas, K. *Abstracts of Specialized Colloque AMPERE and Alexander von Humboldt Workshop: "Advanced Materials as Studied by Spectroscopic and Diffraction Techniques"*, September 16 to September 21, 2006, Vilnius, Lithuania; p 7.

(62) Greer, S. C.; Das, B. K.; Kumar, A.; Gopal, E. S. R. *J. Chem. Phys.* **1983**, *79*, 4545-4552.

(63) Fisher, M. E.; Orkoulas, G. *Phys. Rev. Lett.* **2000**, *85*, 696-699.

(64) Cerdeirina, C. A.; Anisimov, M. A.; Sengers, J. V. *Chem. Phys. Lett.* **2006**, *424*, 414-419.

(65) Orgin Software, http://www.OriginLab.com.